Journal of Applied Mechanics and Technical Physics, Vol. 43, No. 1, pp. 103–108, 2002

MODEL OF SPONTANEOUS CRYSTALLIZATION OF A THIN MELTED LAYER BROUGHT INTO CONTACT WITH A MASSIVE SUBSTRATE

A. I. Fedorchenko and A. A. Chernov

UDC 537.525.1:621.793.7

A model of spontaneous crystallization of a thin melted metal layer brought into contact with a massive substrate is proposed. With invoking the Kolmogorov composite crystallization theory, the model allows one to predict the size distribution of crystallites across the layer, which provides a possibility of controlling the microstructure of the solidifying layer through a proper choice of substrates.

Introduction. Considerable recent attention has been focused on the development of new production methods for nanocrystalline materials (NM) and on studying their properties [1, 2]. The interest in this research field was stimulated by some specific properties of the nanocrystalline state, not displayed by any other materials. For instance, a decrease in the grain size to nanometer values was found to increase the hardness and yield strength of NM by a factor of 4–5 [2, 3].

Nowadays, powder and film technologies are among the main methods used to produce NM. Powdered NM normally contain large pores that largely deteriorate the properties of materials to be synthesized. The film technologies, which include quenching of thin melted layers, are free of this drawback. However, whereas the grain size is pre-determined by the dispersion of the powder used and the grain-size spectrum is rather uniform in compacting ultra-fine powders, the microstructure of layers undergoing solidification in film technologies depends on process regime parameters and on the properties of melt and substrate materials. It is known that, at high cooling rates (greater than 10^3 K/sec), the homogeneous-nucleation condition holds for pure melts; hence, to predict the microstructure of the solidified layer, one has to solve, using the homogeneous-nucleation and composite crystallization theory, a conjugate problem about conductive heat transfer between the melted layer and the massive substrate. The present work was aimed at solving this problem.

Formulation of the Problem. We consider spontaneous crystallization of a thin melted metal layer brought into contact with a massive substrate. The z axis with the origin at the free surface of the melted film is directed inside the substrate. In this case, the boundary-value problem may be formulated as follows:

$$\rho_p c_p \frac{\partial T_p}{\partial t} = \lambda_p \frac{\partial^2 T_p}{\partial z^2} + Q, \qquad \rho_b c_b \frac{\partial T_b}{\partial t} = \lambda_b \frac{\partial^2 T_b}{\partial z^2}. \tag{1}$$

Here ρ, c, and λ are the density, specific heat capacity, and thermal conductivity, respectively, $Q = \rho_p L_p \, d\eta/dt$ is the amount of heat released during crystallization by spontaneously formed nuclei, L_p is the specific melting heat of the melt substance, and η is the mass fraction of crystallinity in the melt; the subscripts p and b refer to the melt and substrate materials, respectively.

We formulate the following initial and boundary conditions:

$$T_p(0, z) = T_p^0, \qquad T_b(0, z) = T_b^0,$$

$$T_p(t, h_p) = T_b(t, h_p), \qquad \left(\lambda_p \frac{\partial T_p}{\partial z}\right)_{z=h_p} = \left(\lambda_b \frac{\partial T_b}{\partial z}\right)_{z=h_p}, \tag{2}$$

$$\left(\frac{\partial T_p}{\partial z}\right)_{z=0} = 0, \qquad (T_b)_{z\to\infty} = T_b^0,$$

Kutateladze Institute of Thermal Physics, Siberian Division, Russian Academy of Sciences, Novosibirsk 630090. Translated from Prikladnaya Mekhanika i Tekhnicheskaya Fizika, Vol. 43, No. 1, pp. 124–130, January–February, 2002. Original article submitted November 20, 2000; revision submitted May 4, 2001.

0021-8944/02/4301-0103 $27.00

where T_p^0 and T_b^0 are the initial temperature of the melt and that of the substrate, respectively, and h_p is the thickness of the melted layer.

The mass fraction of crystallinity in the melt η is given by the Kolmogorov theory of composite crystallization kinetics [4]:

$$\eta(t) = \frac{V(t)}{V} = 1 - \exp\left(- \int\limits_0^t J(x) V_c(t-x)\, dx \right). \tag{3}$$

Here V is the initial volume, $V(t)$ is the volume of the substance that has already solidified, $J = J(\Delta T)$ is the nucleation frequency, $V_c(t;x) = \dfrac{4\pi}{3}\Big(\displaystyle\int\limits_x^t v_c(\tilde{x})\, d\tilde{x} \Big)^3$ is the volume of a growing center that appeared in the melt at the moment $t = x$, $v_c = K\Delta T$ is the crystallite growth rate, K is a kinetic factor, $\Delta T = T_{\rm m} - T$ is the melt overcooling, and $T_{\rm m}$ is the melting point of the melt substance. We determine the homogeneous nucleation frequency as described in [5]:

$$J = N_a C \exp\Big(- \frac{U}{k_{\rm B} T} \Big) \exp\Big(- \frac{16\pi}{3} \frac{\sigma^3 T_{\rm m}^2}{\Delta H_f^2\, \Delta T^2\, k_{\rm B} T} \Big).$$

Here N_a is the total number of atoms (molecules) per unit volume, $C = (2d_a/h)(\sigma k_{\rm B} T)^{1/2}$, d_a is the atomic diameter, $k_{\rm B}$ is the Boltzmann constant, h is the Planck constant, σ is the surface tension at the melt–crystal interface, and ΔH_f is the specific (per unit volume) phase-transition heat.

The total number N_c of crystallization centers formed during the time t in a unit volume is given by the expression [4]

$$N_c(t) = \int\limits_0^t J(x)(1 - \eta(x))\, dx. \tag{4}$$

We introduce the dimensionless variables $\theta = T/T_p^0$, $\zeta = z/h_p$, and $\tau = a_p t/h_p^2$, where a is the thermal diffusivity. Then, problem (1), (2) acquires the following form:

$$\frac{\partial \theta_p}{\partial \tau} = \frac{\partial^2 \theta_p}{\partial \zeta^2} + f(\tau, \zeta); \tag{5}$$

$$\frac{\partial \theta_b}{\partial \tau} = a_{b,p} \frac{\partial^2 \theta_b}{\partial \zeta^2}; \tag{6}$$

$$\theta_p(0, \zeta) = 1, \qquad \theta_b(0, \zeta) = \theta_b^0; \tag{7}$$

$$\theta_p(\tau, 1) = \theta_b(\tau, 1), \qquad \Big(\frac{\partial \theta_p}{\partial \zeta} \Big)_{\zeta = 1} = \lambda_{b,p} \Big(\frac{\partial \theta_b}{\partial \zeta} \Big)_{\zeta = 1}; \tag{8}$$

$$\Big(\frac{\partial \theta_p}{\partial \zeta} \Big)_{\zeta = 0} = 0, \qquad \theta_b(\tau, \zeta \to \infty) = \theta_b^0. \tag{9}$$

Here $f(\tau, \zeta) = {\rm Ku}\, \theta_m\, d\eta/d\tau$, ${\rm Ku} = L_p/(c_p T_m)$ is the Kutateladze criterion, $\theta_m = T_{\rm m}/T_p^0$, $\theta_b^0 = T_b^0/T_p^0$, $a_{b,p} = a_b/a_p$, and $\lambda_{b,p} = \lambda_b/\lambda_p$.

System (5)–(9), together with expressions (3) and (4), uniquely describes the crystallization kinetics and allows one to predict the microstructure of the layer after its complete solidification, i.e., find the distribution of the mean crystallite size over the layer thickness. This system can be only solved numerically.

Numerical Algorithm and Results. To construct a suitable finite-difference scheme, we use the control-volume approach. We divide the time interval $[0, 1]$ into M, and the space interval $[0, 1]$ into N sublayers. We choose a substrate cross section ζ_b, in which condition (9) is imposed, such that the heat wave has not yet reached this cross section for the total solidification time of the melt: $\zeta_b - 1 \gg \sqrt{a_{b,p}\tau_{\rm cr}}$, where $\tau_{\rm cr} = a_p t_{\rm cr}/h_p^2$ ($t_{\rm cr}$ is the total crystallization time of the melt). Assuming the mesh widths along the coordinate ζ in the substrate and in the melt to be identical, we obtain the relation $L/N \gg \sqrt{a_{b,p}\tau_{\rm cr}}$, where L is the total number of nodes along ζ in the substrate. The integer index i refers to the center of the volume, while the fractional indices $i \pm 1/2$ to its faces.

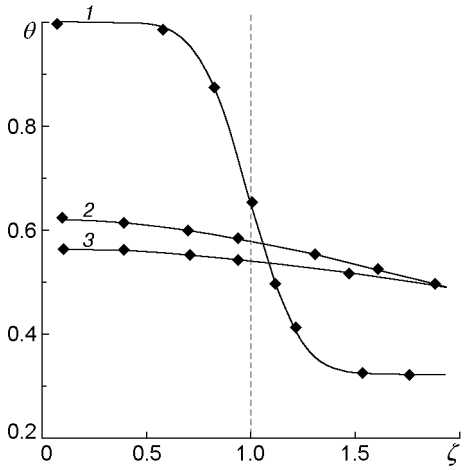

Fig. 1. Temperature-field dynamics in melted aluminum on an aluminum substrate in the absence of solidification for $\tau = 0.02$ (1), 1.46 (2), and 2.32 (3): the solid curves refer to the analytical solution and the points refer to the numerical simulation results.

Integrating Eqs. (5) and (6) over the spatial–time volume $(\zeta_{i-1/2}, \zeta_{i+1/2})(\tau_j, \tau_{j+1})$ with allowance for their respective boundary conditions (8) and (9), we have the following system of finite-difference equations:

— for internal volumes,

$$(\theta_{p\,i}^{j+1} - \theta_{p\,i}^{j})M - (\theta_{p\,i+1}^{j} - 2\theta_{p\,i}^{j} + \theta_{p\,i-1}^{j})N^2 - f_i^j = 0 \qquad (i = 2, 3, \ldots, N-1),$$

$$(\theta_{b\,i}^{j+1} - \theta_{b\,i}^{j})M - a_{b,p}(\theta_{b\,i+1}^{j} - 2\theta_{b\,i}^{j} + \theta_{b\,i-1}^{j})N^2 = 0 \qquad (i = N+2, N+3, \ldots, N+L-1);$$

— for near-boundary volumes,

$$(\theta_{p\,1}^{j+1} - \theta_{p\,1}^{j})M - (\theta_{p\,2}^{j} - \theta_{p\,1}^{j})N^2 - f_1^j = 0, \qquad \theta_{b\,N+L}^{j+1} = \theta_b^0,$$

$$(\theta_{p\,N}^{j+1} - \theta_{p\,N}^{j})M - (\theta_{p\,N-1}^{j} - 3\theta_{p\,N}^{j} + 2\theta_{p\,N+1/2}^{j})N^2 - f_N^j = 0,$$

$$(\theta_{b\,N+1}^{j+1} - \theta_{b\,N+1}^{j})M - a_{b,p}(\theta_{b\,N+2}^{j} - 3\theta_{b\,N+1}^{j} + 2\theta_{b\,N+1/2}^{j})N^2 = 0.$$

The initial conditions (7) acquire the form $\theta_{p\,i}^0 = 1$, $\theta_{p\,N+1/2}^0 = 1$, $\theta_{b\,i}^0 = \theta_b^0$, and $\theta_{b\,N+1/2}^0 = \theta_b^0$. It can be easily shown that, for conjugation conditions (8) to be automatically satisfied, the following conditions must be fulfilled:

$$\theta_{p\,N+1/2}^{j} = \theta_{b\,N+1/2}^{j} = \frac{\theta_{p\,N}^{j} + \lambda_{b,p}\theta_{b\,N+1}^{j}}{1 + \lambda_{b,p}} \qquad (j = 1, 2, \ldots, M).$$

The fact that crystallization in different cross sections proceeds at different overcoolings constitutes the main distinctive feature of the problem. For this reason, both the mass fraction of crystallinity and the total number of centers formed depend parametrically on ζ. If the cooling rate (and the nucleation frequency) is high, then the nucleation centers formed at the initial time rapidly cease the overcooling, thus diminishing the nucleation frequency, and the total number of nucleation centers remains almost unchanged up to the moment at which the layer gets completely solidified. Knowing the total number $N_{ci}(t_{\rm cr})$ of crystallization centers formed in the ith sublayer by the moment of complete solidification of the whole melt layer, one can determine the mean crystallite radius r_i in the given sublayer by the formula $r_i = (3/(4\pi N_{ci}(t_{\rm cr})))^{1/3}$ and, in this manner, find the size distribution function $r(\zeta)$ of the crystallites across the whole layer.

To calculate the integrals in formulas (3) and (4), we used the rectangular formula at each integration step over time. The smallest discretization number of the melted layer $N_{\min}$ was chosen such that the results were identical at $N = 2N_{\min}$ and $N = N_{\min}$. This condition was fulfilled at $N =$ 10–20. The values of L varied within the range of $(50–100)N$. The time step was determined from the stability condition for explicit schemes $N^2/M < 1/2$ [6]. This condition was reliably fulfilled at $M = 1000$.

The computations were carried out for aluminum and copper melted layers on various substrates. The initial melt temperature in all cases was set identical to the melting point of the melt substance ($T_p^0 = T_m$) and the initial

TABLE 1

Material	T_m, K	ρ, kg/m^3	λ, W/(m · K)	c, J/(kg · K)	K, m/(sec · K)	ΔH_f, 10^9 J/m^3	σ, J/m^2	d_a, 10^{-10} m	U, 10^{-20} J/mole
Al	933	2700	209	880	0.049	0.975	0.093	2.67	4.15
Cu	1356	8930	384	390	0.02	1.80	0.18	2.38	6.60
Fe	1530	7880	74	45	—	—	—	—	—

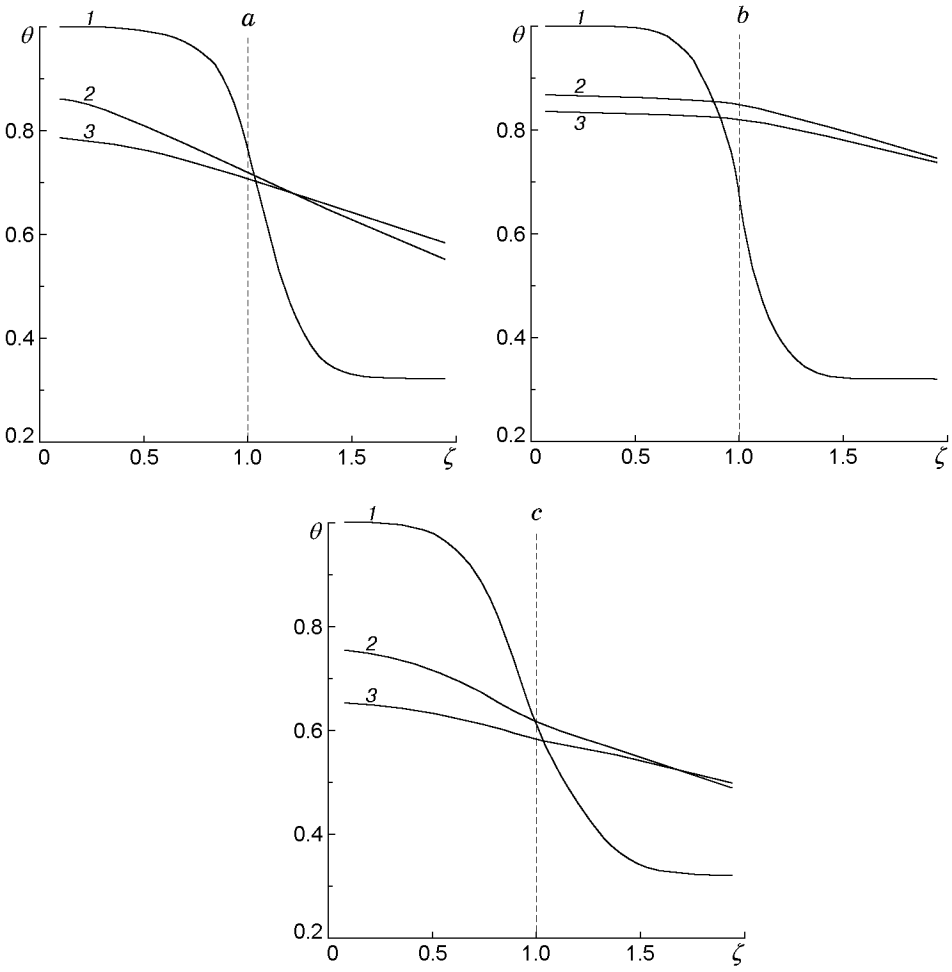

Fig. 2. Temperature-field dynamics during crystallization: (a) aluminum melt on an aluminum substrate for $\tau = 0.02$ (1), 1.46 (2), and 2.32 (3); (b) aluminum melt on an iron substrate for $\tau = 0.02$ (1), 5.65 (2), and 6.71 (3); (c) copper melt on a copper substrate $\tau = 0.04$ (1), 1.37 (2), and 1.82 (3).

substrate temperature was $T_b^0 = 300$ K. The characteristics of substances used in the present study are indicated in Table 1. The values of the kinetic factor K were borrowed from [7].

The results of a test numerical study of conjugate heat transfer between the melted layer and the substrate in the absence of crystallization are depicted by Fig. 1. These results are seen to well agree with the analytical solution [8].

Figure 2a–c shows the simulation data that illustrate the temperature-field dynamics in aluminum melts on aluminum and iron substrates and in copper melts on a copper substrate, respectively. It is seen that the intense heat release due to the increase in the mass fraction of crystallinity causes the temperature fields to change dramatically. For instance, under conditions without crystallization, the temperature at the melt–substrate interface decreases to 0.58 by the moment $t = 1.46$ (see Fig. 1), and it increases to 0.72 by the same time during crystallization (see Fig. 2a). Such a profound increase in temperature is caused by high values of the nucleation frequency and kinetic constant of aluminum. It is just this property of aluminum that explains its aptitude to crystallization

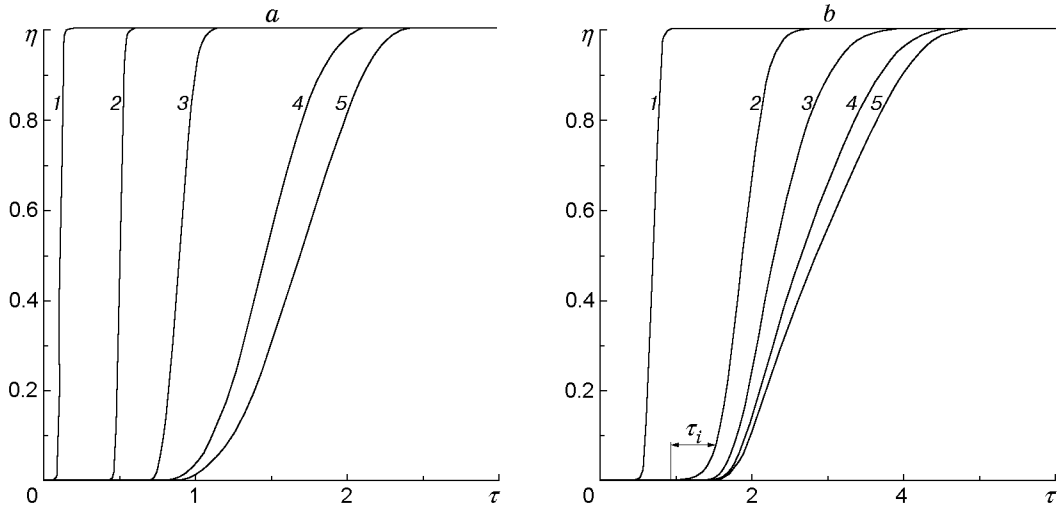

Fig. 3. The dependence of the mass fraction of crystallinity in the aluminum melt in its various cross sections on aluminum substrate (a) and iron substrate (b) for $z = 0.85$ (1), 0.65 (2), 0.45 (3), 0.25 (4), and 0.05 (5).

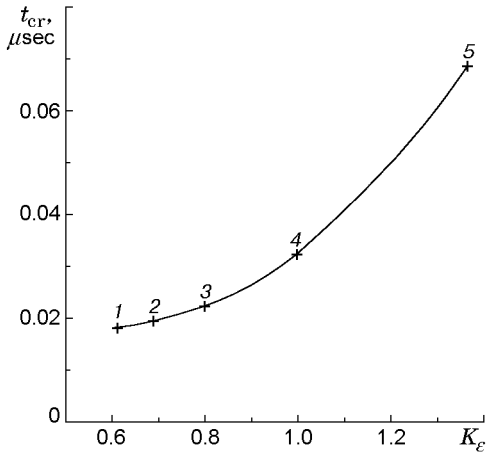

Fig. 4. Total solidification time of a 1 μm-thick aluminum-melt layer versus relative thermal activity parameter K_ε on copper (1), silver (2), gold (3), aluminum (4), and iron (5) substrates.

according to the equilibrium mechanism and the fact that amorphous aluminum remains hard to obtain [7]. It is seen from Fig. 2b that the comparatively low thermal conductivity of the iron substrate makes the overcooling rapidly decrease and, hence, leads to establishment of solidification conditions close to equilibrium. Unlike aluminum, the copper melt on a copper substrate crystallizes at very high values of overcooling (see Fig. 2c) caused both by the high thermal conductivity of the copper substrate and by comparatively low nucleation frequency of the copper melt.

Figure 3 shows the growth dynamics of the mass fraction of crystallinity in various sections of the aluminum melt on aluminum and iron substrates. It is seen that, in both cases, a planar crystallization front is immediately formed near the substrate (in the cross section $z = 0.85$). In the case of the aluminum substrate, this front remains planar up to the cross section $z = 0.45$. In the case of iron substrate, the crystallization front looses its planarity already in the cross section $z = 0.65$, since the fraction of crystallinity increases over rather a long time interval, from $t = 1$ to $t \simeq 2.5$. The latter is related to an intense heat release of the aluminum melt due to the high nucleation frequency and to the low heat-removal capacity of the iron substrate. Therefore, the duration of solidification of the aluminum melt layer on the iron substrate is nearly twice that of the same melt on the aluminum substrate.

An examination of solidification of each sublayer allows the following conclusions to be drawn. At the beginning of the process, the fraction of crystallinity is very small and increases slowly (small number and small overall surface area of growing crystallites). This time interval τ_i (see Fig. 3) is called an incubation period. Then,

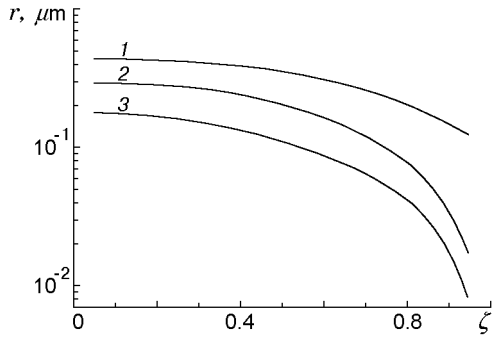

Fig. 5

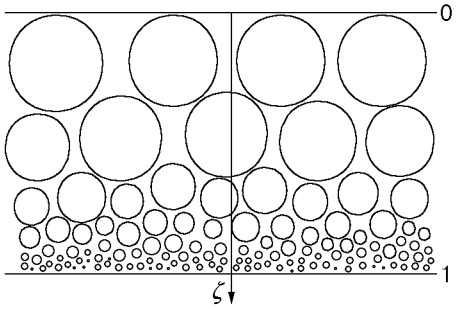

Fig. 6

Fig. 5. Size distribution of crystallites across the solidified aluminum-melt layer ($h_p = 1$ μm) on iron (1), aluminum (2), and copper (3) substrates.

Fig. 6. Schematic of the size distribution of crystallites across the solidified aluminum-melt layer ($h_p = 1$ μm) on the aluminum substrate.

the crystallization rate sharply increases and remains unchanged until the volume of the noncrystallized substance reaches 10–20% of the initial volume. Under these conditions the initial overcooling rapidly diminishes, and the homogeneous-nucleation frequency accordingly decreases. As a result, the fraction of crystallinity increases more slowly.

The total crystallization time as a function of the relative thermal activity parameter $K_\varepsilon = \sqrt{\lambda_p \rho_p c_p / (\lambda_b \rho_b c_b)}$ is shown in Fig. 4. It follows from these data that the total crystallization time strongly depends on the parameter K_ε. For instance, as the parameter K_ε increases from 0.6 for the Al–Cu pair to 1.4 for the Al–Fe one, i.e., by a factor of 2.3; the time required for complete crystallization increases almost by 3.8 times.

The model proposed allowed us to predict the cross-sectional size distribution of crystallites in melt layers. For a 1 μm-thick aluminum layer on iron, aluminum, or copper substrates, the data obtained are plotted in Fig. 5. In all the three cases, the largest scatter in the values of r is observed near the substrate, where the overcooling is most intense and, hence, the nucleation frequency is highest. Since the number density of nucleation centers in this regions is high, their further growth is arrested by near-by crystallites. As the crystalline mass increases owing to released latent phase-transition heat, the overcooling decreases, and the nucleation frequency accordingly decreases. As a consequence, the limiting crystallite size increases. The smallest scatter in r observed for the iron substrate with low thermal conductivity substantially increases as the parameter K_ε decreases. The microcrystalline structure across the solid layer corresponding to curve 2 of Fig. 5 is shown in Fig. 6. Thus, a proper choice of the substrate material allows one to precisely control the microstructure of the layer after its solidification in order to ensure either its sharp inhomogeneity in the case of substrates with high thermal conductivity (curves 2 and 3 in Fig. 5) or an almost uniform distribution in the case of substrates with low thermal conductivity (curve 1 in Fig. 5).

REFERENCES

1. R. A. Andrievskii and A. M. Glezer, "Dimensional effects in nanocrystalline materials. 1. Structural features. Thermodynamics. Phase equilibria. Kinetic phenomena," *Fiz. Metal. Metaloved.*, **88**, No. 1, 50–73 (1999).
2. R. A. Andrievskii and A. M. Glezer, "Dimensional effects in nanocrystalline materials. 2. Mechanical and physical properties," *Fiz. Metal. Metaloved.*, **89**, No. 1, 91–112 (2000).
3. M. A. Shtremel', *Strength of Alloys* [in Russian], Vol. 2, Inst. of Steel and Alloys, Moscow (1997).
4. A. N. Kolmogorov, "On the statistical theory of metal crystallization," *Izv. Akad. Nauk SSSR, Ser. Mat.*, No. 3, 355–359 (1937).
5. B. Ya. Lyubov, *Theory of Crystallization in Large Volumes* [in Russian], Nauka, Moscow (1975).
6. P. J. Roache, *Computational Fluid Mechanics*, Hermosa, Albuquerque (1976).
7. A. I. Fedorchenko, "Phase transition upon solidification from a liquid state," *Prikl. Mekh. Tekh. Fiz.*, **42**, No. 1, 108–114 (2001).
8. A. V. Lykov, *Thermal-Conduction Theory* [in Russian], Vysshaya Shkola, Moscow (1967).